Archives of Current Research International
3(4): 1-12, 2016, Article no.ACRI.25848
ISSN: 2454-7077

SCIENCEDOMAIN *international*
www.sciencedomain.org

Ammonia Decomposition at Titanium Oxide Nanotube Photosensitive Anode

Yong X. Gan[1*], Jeffrey Zampell[1], Ryan N. Gan[2], Juan C. Miranda[1], Marla Lopez[1], Andrew Vitaljic[1], Bruce Y. Decker[1], James L. Smith[3] and Jimmie C. Oxley[3]

[1]Department of Mechanical Engineering, California State Polytechnic University, Pomona, 3801 West Temple Avenue, Pomona, CA 91768, USA.
[2]Diamond Bar High School, 21400 Pathfinder Road, Diamond Bar, CA 91765, USA.
[3]Department of Chemistry, University of Rhode Island, 45 Upper College Road, Kingston, RI 02881, USA.

Authors' contributions

This work was carried out in collaboration between all authors. Author YXG managed the project, designed the study and wrote the first draft of the manuscript. Authors JZ, RNG, JCM, ML, AV and BYD performed the literature search, carried out the experiments and analyzed the data. Authors JLS and JCO advised the study. All authors read and approved the final manuscript.

Article Information

DOI: 10.9734/ACRI/2016/25848
Editor(s):
(1) Sung-Kun Kim, Department of Natural Sciences, Northeastern State University, USA.
Reviewers:
(1) Anonymous, National Polytechnic Institute, Mexico.
(2) Raahul Krishna, University of Mumbai, India.
Complete Peer review History: http://sciencedomain.org/review-history/14151

Original Research Article

Received 22nd March 2016
Accepted 8th April 2016
Published 14th April 2016

ABSTRACT

Kinetic behavior of ammonia decomposition at titanium dioxide nanotube photosensitive anode was studied. Ammonia was dissolved into water to form solutions with difference concentrations. The ammonia concentration ranges from 0.025 wt% to 10 wt%. Time-dependent open-circuit potential was measured to examine the photochemical response of the cell. The ammonia decomposition behavior was confirmed by measuring the decrease in pH values of the solutions. In addition, the kinetic behavior of ammonia decomposition was characterized under the actions of both ultra violet light irradiation and polarization. The current density values at the titanium dioxide nanotube anode during anodic polarization and UV light irradiation tests were used to compare the ammonia decomposition rates associated with photon excitation and polarization. The double–layer capacitance was estimated as high as 35 F/m^2 indicating the excellent charge storing capability of

**Corresponding author: Email: yxgan@cpp.edu;*

the nanotube photosensitive anode. The effect of ammonia concentration on the open-circuit potential was also observed. In the lower ammonia concentration range, the change in the open circuit potential increase with the increasing in the ammonia concentration. Interestingly, in the higher concentration range from 2.5 wt% to 10 wt%, the change in the open circuit potential reveals a reversed trend.

Keywords: Nanostructures; oxides; electrochemical techniques; surface properties.

1. INTRODUCTION

Ammonia released from fertilizers and animal waste in agriculture land is considered as a hazardous material. In addition to originating from the agriculture, ammonia and ammonium compounds as explosive substances could come from the extensive mining and construction activities. Ammonia and ammonium compounds dissolved in water are harmful for many species such as fish. As nitrogen-containing pollutants, they are nutrients promoting algae growth in natural water. Thus, there is a need to decompose the ammonia and ammonium substances in environment. Cleaning wastewater via photochemical reactions attracts significant research interest. Nanostructured biophotofuel cell systems have been considered for both energy generation and environment cleaning [1]. The main research focus is on designing novel biophotofuel cells consisting of a nanoporous material as the photosensitive anode at which biomass decomposition occurred. Besides the photosensitive anode, a low-hydrogen overpotential metal Pt, or Ru is used as the cathode for hydrogen generation [2]. The uniqueness of the system lies in the multiple functions of the cell. It can generate electricity and produce hydrogen from bio-hazardous substances under sunshine [3]. Meanwhile, noxious gases such as ammonia released from biowaste may be decomposed at the photosensitive anode and pure water can be generated for reuse in the cathode region [4,5]. In order to prepare such key components in the system which allows the electron-hole pair separation under irradiation, and decomposes biomass, semiconducting substances such as pure and doped-TiO_2 nanotubes were made into photosensitive electrode with regularly aligned nanopores [6]. Due to the nanoporous array structure of the newly developed electrode, high surface areas can be obtained. However, the photochemical fuel cells have to be tested and validated in view of electricity and hydrogen generation from biomass under solar rays, noxious gas decomposition, and clean water regeneration.

Various approaches are introduced for ammonia decomposition or denitrification including pure metal chemical catalysis approach, electrochemical approach, photochemical and photo-electrochemical method. In metal catalyst approach, an active catalyst is set on a support. A decomposition promoter may also be used. As reported in [7] on generation of hydrogen from ammonia decomposition using fuel cells, Ru is considered as the most active catalyst. While carbon nanotubes (CNTs) have been found as the most effective support. KOH is taken as the best promoter. Early work shows that the active metallic components including Ru, Rh, Pt, Pd, Ni, Fe and various support materials such as carbon nanotubes, active carbon, alumina, magnesium oxide, zirconia, titanium oxide affect the catalytic decomposition of ammonia for hydrogen generation [8]. High voltage assisted metal catalysis approach using an AC charge reactor for decomposing ammonia was also proposed [9]. Nickel, stainless steel (SS) and copper tubular electrodes were used. It was found that the high-voltage electrodes showed higher activity than the ground electrodes.

In the photo-electrochemical approach, oxide catalysts are considered as the active components for ammonia decomposition. For example, RuO_2 and IrO_2 as the active components were tested under different electrochemical and photochemical catalysis conditions [10]. It confirmed that the photochemical process showed higher ammonia degradation rate than the electrochemical approach. Due to the action of the ultraviolet light, the average current efficiencies of ammonia decomposition were increased by 1.5 and 1.7 times respectively for RuO_2 and IrO_2. Oxides may be in self-support form or supported by other materials including carbon nanotubes as shown in both [11] and [12]. In addition to RuO_2 and IrO_2, other oxides such as CuO, CoO, NiO, TiO_2, V_2O_5, MoO_3 are also used as the active

photo-catalysts [13]. In [14], TiO_2, was taken as the major component, while NiO, V_2O_5, MoO_3 were added into TiO_2 to enhance the photo-catalysis activities. TiO_2 loaded with various metals including noble and transition ones [15-17], metal and nonmetal mixtures [18], metal and oxide mixtures [19,20] have extensively been studied for increasing the light absorbing capability. The absorption band for TiO_2 can be extended from UV range to visible light range by incorporating metals, nonmetals or ceramics [21].

The photocatalytic property of well-aligned TiO_2, nanotube arrays attracts interest for ammonium decomposition as shown in [22]. The reasons for using titanium dioxide nanotubes are multifold. They can vertically grow on the Ti metal sheet to form the array structure [23]. The nanotubes can be doped to become conductive and have stable adhesion to the metal substrate [24]. They have large specific surface area for incident light harvesting and for surface catalytic reaction and the effectiveness for the treatment of biomass and various organic pollutants including nitro-aromatic explosive has been demonstrated [25,26]. Compared with other forms of photochemical catalysts, the nanotube catalyst has some advantages. For example, titanium oxide nanoparticle catalyst tends to from aggregates, leading to degradation of catalysis. While titanium oxide film catalyst has much less surface area than the nanotube one, resulting in low photochemical catalytic efficiency.

In this work, titanium dioxide nanotubes (TiO_2 NTs) were prepared through electrochemical oxidation of pure Ti sheet in an ammonium fluoride and ethylene glycol-containing solution. Scanning electron microscopy was used to analyze the morphology of the nanotubes. The average diameter, wall thickness and length of the as-prepared TiO_2 NTs were determined. Photosensitivity of the anode made from the highly ordered TiO_2 NTs with good photo-catalytic property was shown by ammonia decomposition tests under ultraviolet (UV) radiation. To understand the ammonia decomposition kinetics, the pH values of the solution before and after UV light irradiation were measured. The photo-electrochemical response of the anode was also tested to examine the ammonia decomposition behavior under the actions of both ultraviolet light irradiation and anodic polarization. The current density at the titanium dioxide nanotube anode during the tests was used to calculate the double-layer capacitance.

2. MATERIALS AND EXPERIMENTAL PROCEDURES

Titanium (Ti) sheet with a thickness of 0.1 mm was used for making the TiO_2 nantotube (NT) array. Ammonia, ammonium fluoride, and ethylene glycol were purchased from Sigma-Aldrich. A solution containing NH_4F, ethylene glycol and water was prepared for growing nanotubes. The DC power supply system for nanotube processing consists of a model 01PHSY 5003 DC unit being connected with an ampere meter in series. Scanning electron microscopy (SEM) was used for morphology observation. A UVL-21 (365 nm, 4 W, 0.16 A) was used to generate UV light. The ammonia decomposition was monitored by measuring the pH value and open circuit potential of the cell.

A two-electrode cell was used for electrochemical oxidization of Ti to form TiO_2 nanotubes at the room temperature of 25°C. The anode was a Ti sheet, and the cathode was a platinum wire. The distance between the two electrodes was 20 mm. The most important processing parameter, operation voltage, was 50.0 V and the electrochemical oxidization time was 2 h. The other related processing parameter, the current density changes with the electrochemical oxidation time. We set the processing parameter, the operation voltage as 50 V because the requirement of the nanotube diameter. It was found that the higher the voltage used, the thicker the nanotubes [21,23]. By optimization, we found that the voltage level of 50 V could control the diameter range of the nanotubes from 100 nm to 200 nm, which provides best photocatalytic property. After the electrochemical oxidization, the nanotube sample was rinsed in water and air dried. The surface of the anode was completely covered by TiO_2 nanotube arrays as revealed by the electron microscopic analysis. After the TiO_2 NTs were prepared, high temperature annealing at 450°C for 2 h was conducted to crystallize the TiO_2. The specimen was cooled down slowly, and it was used to make the photosensitive anode for the cell. Solutions containing different concentration of ammonia were made for photochemical decomposition tests using the nanostructured anode.

3. RESULTS AND DISCUSSION

3.1 TiO_2 Nanotube Array Preparation and the Configuration of Photoelectro-chemical Cell

Fig. 1 shows the schematic of the cell for TiO_2 nanotube array processing, the surface morphology of the anode with the processed TiO_2 nanotube array and the chemical composition of the nanotubes. Fig. 1(a) illustrates the configuration of the two-electrode cell in the one-compartment form. The anode is the TiO_2 nanotube arrays on Ti. The cathode is Pt. The main reaction at the cathode is hydrogen generation. Reactions at the anode and in the solution cause the formation of the nanotubes. Fig. 1(b) is an SEM image showing the open end of the nanotubes. The outer diameter of the TiO_2 nanotubes is about 120 nm. The wall thickness is around 20 nm. Elemental analysis shows that there are four elements, Ti, O, F and Al. The major elements are Ti and O. The minor ones are Al and F. F comes from the residue of the fluorine ion based solution and Al is considered as the purity in the Ti sheet. The atomic ration of Ti to O is 33.67:63.65 (shown in the inset of Fig. 1c), which is approximately equal to 1:2. This indicates that the stoichiometric compound TiO_2 is the major chemical composition of the titanium oxide nanotube. In Fig. 2, the configuration of the three-electrode cell in the one-compartment form is demonstrated. The anode consists of the TiO_2 nanotube array on the Ti substrate. The cathode is a Pt wire. The reference electrode is Ag/AgCl soaked in 3 M KCl solution. The main reaction at the anode causes the decomposition of ammonia is monitored by the pH meter. By frequent measuring the decreasing in the pH value, the drop in alkalinity, which is associated with the decrease of ammonia concentration in the solution can be confirmed. The electron generation at the anode is reflected by the electricity generated in the external circuit of the cell. This was measured by a CHI 440C Electrochemical Analyzer as shown in the top part of Fig. 2.

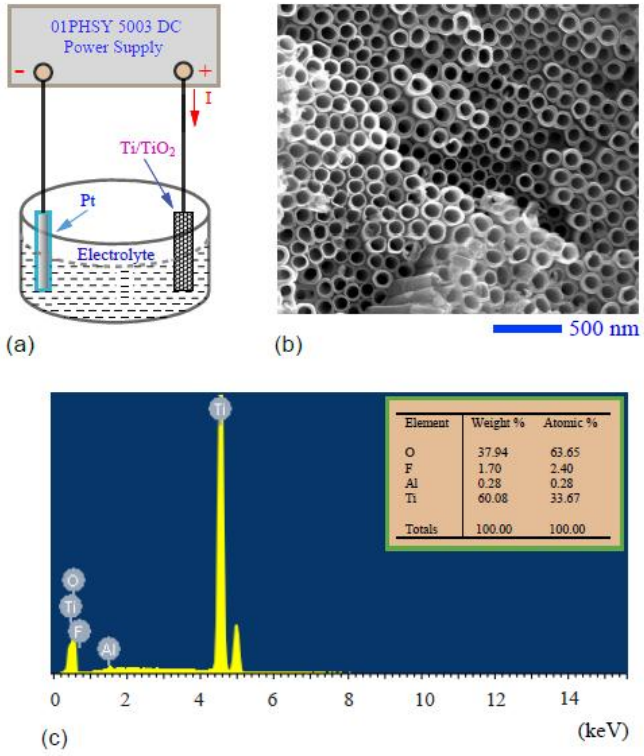

Fig. 1. Schematic of titanium dioxide nanotube processing and microstructure observation: (a) illustration of the electrochemical oxidization cell, (b) scanning electron microscopic image showing the top view of the titanium dioxide nanotubes, and (c) composition analysis results from the energy dispersive X-ray diffraction experiment

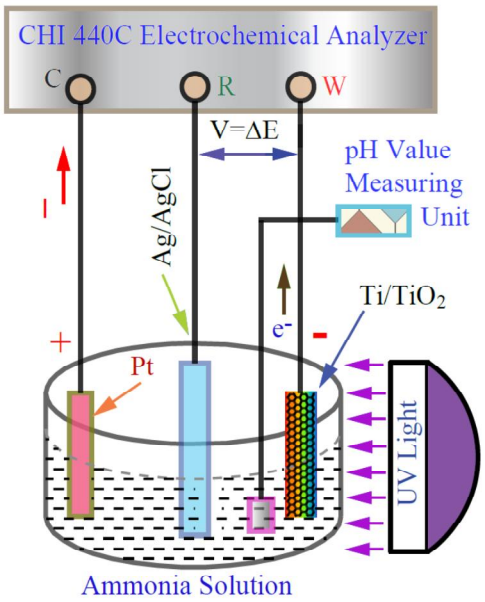

Fig. 2. Test facility set-up for the ammonia decomposition at the TiO_2 photosensitive anode

3.2 Photosensitivity of the Nanotube

The solutions containing different concentrations of ammonia were inducted into the one-compartment photochemical cell. UV radiation was generated by the light source. In general, only the anode is necessary to be kept under the irradiation. It is observed that there is a voltage across the two electrodes of the cell. The open circuit potential was measured as a function of time using the CHI 440C Electrochemical Analyzer. Also recoded are the dynamic response data when the UV light ON and OFF were switched.

Fig. 3(a), (b) and (c) show the open circuit potential (E) v.s. time (t) curves obtained from the tests on the solutions containing 0.5 wt%, 0.25 wt% and 0.025 wt% ammonia, respectively. Fig. 3(a), (b) and (c) show that when the UV light is ON, the voltage at the photosensitive anode drops. When the UV light is OFF, the voltage goes up. This is because the main photosensitive reaction at the anode, which is expressed as:

$$2TiO_2 + hv\ (\text{UV light}) \rightarrow TiO_2(h^+) + TiO_2(e^-) \quad (1)$$

where h^+ and e^- stand for hole and electron, respectively. The electrons accumulate at the anode. Due to the nature of negative charge of the electrons, the potential of the nanotube anode drops when the UV light is ON. While the UV light is OFF, the dissipation of the electrons through the external circuit allows the potential to come back to the equilibrium.

In the solution, ammonia decomposes through the combination with the holes. The possible reaction mechanism is that the ammonia reacted with hydroxide ion while combined with the holes to generate nitrogen gas and water as shown in Equation (2).

$$2NH_3 + 6OH^- + 6h^+ \rightarrow N_2\uparrow + 6H_2O \quad (2)$$

In order to confirm the above reaction mechanism, measuring the pH value of the solution in the anode region before the UV irradiation and after the irradiation was conducted. The total irradiation time is 30 min. Fig. 4 shows the results from the solutions with two different concentration of ammonia. It is evident that immediately after the UV irradiation, the pH value dropped. For the solution contains 0.025 wt% of ammonia, the pH value was about 9.89. After the photochemical reaction under UV irradiation, the pH value decreased to 8.59. Similarly, for the solution with ammonia concentration of 0.05 wt%, the initial pH value was 9.92 before the UV irradiation. After the irradiation, its pH value dropped into 8.49. The decreasing in the alkalinity of the solution directly proves the ammonia decomposition through the consumption of the hydroxide ion.

However, the decreasing in the alkalinity of the solution can be suppressed by the cathode reaction. This is the explanation that the pH values of the solutions would not go to the acidic range even if the irradiation time is even longer. At the cathode, the oxygen absorption as expressed in [27,28] (Equation (3)) should be the main reaction. This reaction generates hydroxyl ion and prevents the pH value of the solution from dropping to the acidic range.

$$2H_2O + O_2 + 4e^- \rightarrow 4OH^- \quad (3)$$

Generally, a photochemical anode may be sensitive to the atmosphere. However, in this study we are testing the anode by putting it in the low concentration ammonia solutions. The influence of the atmosphere should be minimum.

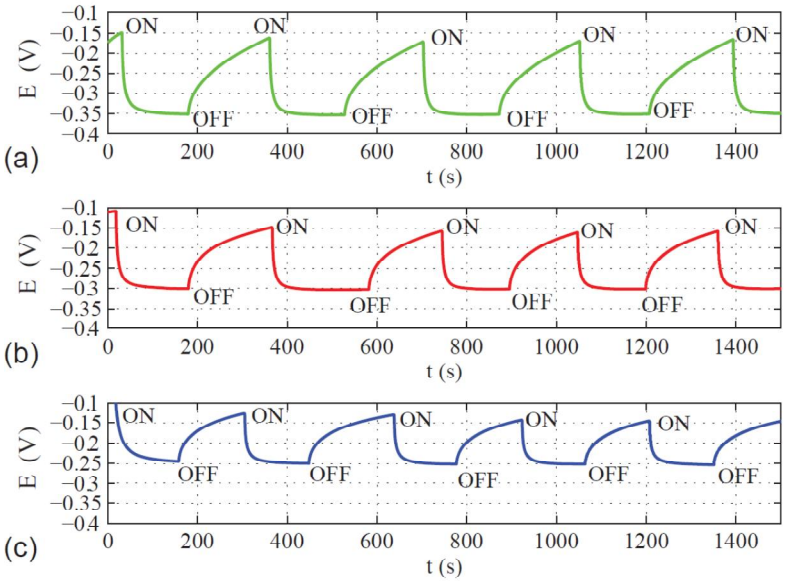

Fig. 3. UV response of the photochemical cell with different ammonia concentrations: (a) 0.5 wt% ammonia, (b) 0.25 wt% ammonia, and (c) 0.025 wt% ammonia

3.3 Kinetics of the Photochemical Reaction

Time-dependent open circuit potential of the nanotube anode was measured. This measurement is similar to the chronopotentiometry except for the current is zero. The time-dependent open circuit potential data were used for analyzing the kinetics of the photochemical reaction. By examining the experimental data, it is found that the kinetics of the photon energy response can be divided into two separated stages, the charging stage and the discharging one. Representative data obtained from the decomposition of ammonia are plotted and shown in Fig. 5. Fig. 5(a) reveals the charging behavior. When the UV light is ON, the voltage at the photosensitive anode drops due to electron generation and accumulation at the photosensitive anode. When the UV light is ON (i.e. in the charging cycle), the change in the anode potential, E_1, is a function of irradiation time, t. Here we assume that t takes the value greater than 1 second because the test time is significantly longer than seconds. Since the photocatalytic reaction is heterogeneous and the electron hole pair generation and recombination are fast processes, the Nernst potential should follow the modified Karaoglanoff's equation [29,30]

$$E_1 = E_0 + \frac{RT}{nF}\ln\left(\frac{\sqrt{\tau}-\sqrt{t}}{\sqrt{t}}\right) \quad (4a)$$

where τ is the transition time, which is constant associated with the charging cycle; E_o is the equilibrium potential, which is about -0.09 V in the charge cycle; R is the gas constant; T is the absolute temperature; F is the Faraday's constant and n is the number of electron in the photoelectrochemical reaction. Generally, τ takes much higher values than the variable t. So the approximation of the above equation (4a) generates

$$E_1 = E_0 + \frac{RT}{2nF}\ln(\tau) - \frac{RT}{2nF}\ln(t) \quad (4b)$$

When the UV light is OFF (i.e. in the discharging cycle), the recovery of the potential is expected as initially shown by the three subplots in Fig. 3. But the discharge cycles shown in Fig. 3 only provide the information that the potential difference is decreasing with the UV light OFF. It is necessary to examine the behavior in more detail so that the discharging kinetics can be seen in a quantitative way. The UV light OFF causes the voltage going up with time t, which can be highlighted by Fig. 5 (b). The time dependent response of the photochemical cell to the UV light can be analyzed as in the stage of charging. However, the function is slightly different as the starting point is E_1 (the immediate potential before the UV light OFF, which takes a negative value) instead of E_0. Therefore, the change in the potential as shown in Fig. 5(b) is a function of the recovery or relaxation time, t, which is in the form as follows:

$$E_2 = E_1 + A\ln(Bt) \quad (5)$$

where *A* is constant related to temperature, gas constant, the number of electron in the reaction; *B* is a constant associated with the relaxation time in the discharging or recovery cycle. The unit of constant *A* is volt, and its value can be determined through the data fitting using Fig. 5(b), which is equal to 0.08829 V. As for the unit of constant *B*, it is dimensionless. The value of *B* can be determined from the data presented in Fig. 5(b) as 0.04138.

3.4 Effect of Ammonia Concentration on the Photosensitivity

The ammonia concentration effect on the photosensitivity can be seen from the drop of the open circuit potential when the UV light is ON or the recovery of the open circuit potential after the UV light is OFF. For example, in the 0.5% in weight of ammonia solution, the open circuit voltage change (ΔE) is about 0.255 V. The 0.25% solution shows the maximum ΔE of 0.24 V. The 0.025% solution shows the least change among the three solutions in the open circuit potential of only 0.17 V.

In order to examine the concentration effect in a wider range, we tested more ammonia solutions. Especially, the ammonia solution with higher concentrations were examined. The highest concentration is 10 wt%. The test results are listed in Table 1. In the lower ammonia concentration range, the change in the open circuit potential increases with the increasing in the ammonia concentration. Interestingly, in the higher concentration range from 2.5 wt% to 10 wt%, the change in the open circuit potential reveals a reversed trend. The possible reason is that in the lower ammonia concentration range from 0.025 wt% to 1.25 wt%, the photochemical reaction is a mass transfer controlled process. The concentration limited or diffusion limited mechanism constrained the reaction rate. With the increasing of the concentration of the ammonia solution, the available ammonia at the photosensitive anode was increased. The electron ejection got more intensive at the anode surface under the photon excitation when it was placed in a higher concentration solution. Therefore the potential of the anode became more negative in the solution with higher ammonia concentration.

On the contrary, in the higher ammonia concentration range from 2.5 wt% to 10 wt%, the reaction as given by Equation (2) associated with the decomposition of ammonia was faster than in the lower concentration solutions (0.025 wt% to 1.25 wt% ammonia).

In order to replenish the OH^- for sustaining the ammonia decomposition, the reduction at the cathode as expressed by Equation (3) was accelerated. The consumption of the electron through the above reaction in the cathode region facilitated the electricity generation and allowed the electrons to move away from the photosensitive anode through the external circuit. That is why the change in the open circuit potential at the anode (ΔE) was decreased with the increasing of the ammonia concentration (in the range from 2.5 wt% to 10 wt%).

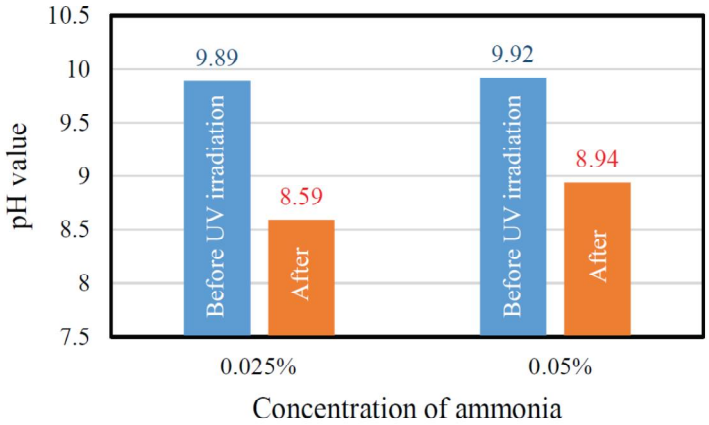

Fig. 4. Comparison of pH values before and after 30 min UV irradiation for two solutions.

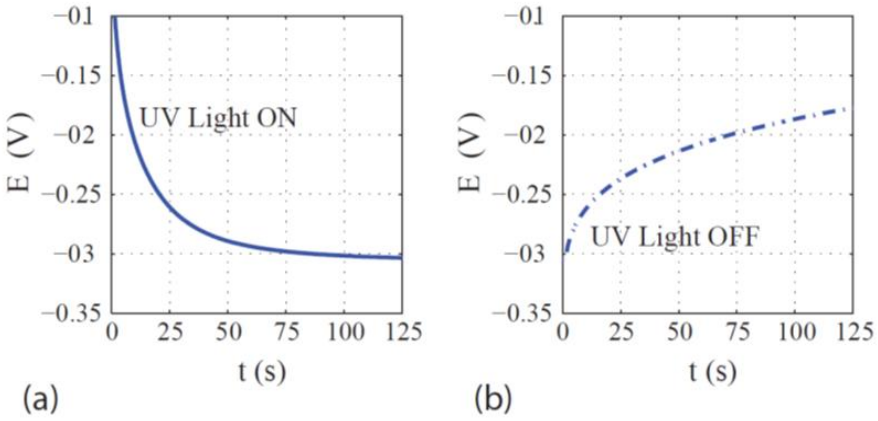

Fig. 5. Time-dependent behavior of the photochemical cell in different phases: (a) UV irradiation, and (b) recovery without UV light

Table 1. Results showing the pH value changes after UV irradiation for 30 min

Sample number	Concentration of ammonia in w.t.%	pH value	OCP Change, ΔE (V)
1	10.0	13.10	0.21
2	7.5	12.98	0.22
3	5.0	12.85	0.27
4	2.5	12.25	0.28
5	1.25	11	0.31
6	1.0	10.63	0.30
7	0.625	10.54	0.26
8	0.5	10.51	0.255
9	0.25	10.40	0.24
10	0.1	10.05	0.21
11	0.05	9.92	0.19
12	0.025	9.89	0.17

3.5 Photo-electrochemical Response

It is interesting to examine the photo-electro-chemical properties of the nanotube anode by imposing bias voltage and exciting with photon energy. Time-dependent electrochemical reaction current at the nanotube anode was measured under the actions of both bias potential and UV irradiation using the CHI 440C Electrochemical Workstation. The scan rate is 0.01 V/s. The cell consisting of three electrodes, TiO_2 nanotube work electrode, Pt counter, and Ag/AgCl reference. The concentration of ammonia is 10 wt% in the cell. The results are shown in Fig. 6. When the bias potential was increased from 0.0 V (vs Ag/AgCl reference electrode) to 0.25 V, the current density increased monotonically. It is noted that the current density was calculated based on the initially surface area of the titanium sheet before the electrochemical oxidization for nanotube processing.

It can be seen form Fig. 6 that for the case without photon energy excitation, the current density changed from 0.15 A/m^2 to 0.35 A/m^2. With the UV irradiation, the photo-electrochemical current changed from 0.5 A/m^2 to 0.7 A/m^2. The difference in the current densities for the two cases, which is about 0.35 A/m^2 reflects the contribution by the photon energy. The higher this value is, the faster the photochemical reaction is. This current density value may also be used to determine the double-layer capacitance C_d during the photochemical reaction as shown below.

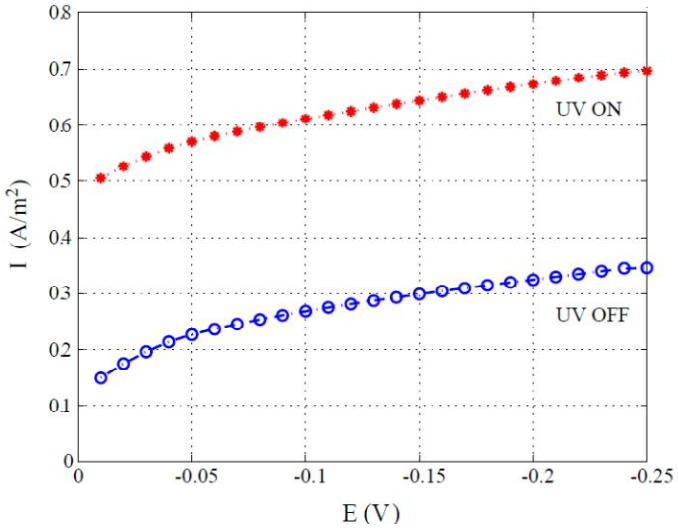

Fig. 6. Current density vs bias potential indicating the photo-electrochemical response of the cell. The concentration of ammonia is 10 wt% in the cell

The charge stored in the double-layer, *Q*, can be expressed as [29]:

$$Q = C_d AE \quad (6)$$

where *A* is the nominal surface area of the photosensitive electrode and *E* the bias potential. The current at the anode, I_a, is:

$$I_a = \frac{dQ}{dt} = C_d A(\frac{dE}{dt}) \quad (7)$$

where $\frac{dE}{dt}$ is the potential scan rate, which is 0.01 V/s in this study.

From Equation (7), the current density, i_a, and the double-layer capacitance, C_d, are correlated by the following equation.

$$i_a = \frac{I_a}{A} = C_d(\frac{dE}{dt}) \quad (8a)$$

Rearranging Equation (8a), the double-layer capacitance, C_d, is given as:

$$C_d = i_a/(\frac{dE}{dt}) \quad (8b)$$

Substituting i_a = 0.35 A/m^2 and $\frac{dE}{dt} = 0.01$ V/s into the Equation (8b), we found that C_d =35 F/m^2.

The value of the double-layer capacitance reflects the capability of storing electrical energy in the Helmholtz layer [30]. Typically, the magnitude of the double-layer capacitance is in the order of 0.1 to 1.0 F/m^2 [31]. From the above calculation, the double layer of the titanium dioxide nanotube anode/ammonia electrolyte has a much higher capacitance. It is more than 35 times higher than the ordinary electrochemical system. Therefore, the charge storing capability of the nanotube photosensitive anode is much higher than that of other systems.

4. CONCLUSIONS

The design, fabrication and characterization of the nanostructured photochemical cell for ammonia decomposition lead to the following conclusions. The titanium dioxide nanotubes (TiO_2 NTs) prepared via electrochemical oxidization of pure Ti in the ammonium fluoride and ethylene glycol-containing solution show UV light sensitivity. It is demonstrated by the fact that the open-circuit potential of the cell decreases under UV irradiation. Scanning electron microscopic analysis reveals that the nanotubes have an average diameter of 120 nm, wall thickness of 20 nm. Composition analysis shows that Ti, O, Al and F are the major elements of the nanotube.

The photochemical cell with the titanium dioxide nanotube array photosensitive anode has been successfully used for decomposing the environmentally hazardous material: ammonia. The ammonia decomposition was confirmed by measuring the decrease in pH values of the solutions. The kinetic behavior of ammonia

decomposition was characterized under the actions of both ultra violet light irradiation and polarization. The current density values at the titanium dioxide nanotube anode during anodic polarization and UV light irradiation tests were used to compare the ammonia decomposition rates associated with photon excitation and polarization. The double–layer capacitance is as high as 35 F/m^2 indicating the excellent charge storing capability of the nanotube photosensitive anode.

The effect of ammonia concentration on the open-circuit potential is studied. In the lower ammonia concentration range, the change in the open circuit potential increases with the increasing in the ammonia concentration. In the higher concentration range from 2.5 wt% to 10 wt%, the change in the open circuit potential shows a reversed trend. This is because in the lower ammonia concentration range (from 0.025 wt% to 1.25 wt%), the photochemical reaction is a mass transfer controlled process. The concentration limited mechanism restrained the reaction rate. With the increasing of the concentration of the ammonia, the available ammonia at the photosensitive anode is increased. The electron ejection becomes more intensive at the anode surface under the photon excitation when it is inserted into a higher concentration solution. Therefore the potential of the anode becomes more negative in the solution with higher ammonia concentration. On the contrary, in the higher ammonia concentration range from 2.5 wt% to 10 wt%, the decomposition of ammonia is much faster than in the lower concentration solutions (0.025 wt% to 1.25 wt% ammonia). In order to replenish the OH^- for sustaining the ammonia decomposition, the reduction at the cathode is accelerated. The consumption of the electron through the reduction reaction in the cathode region facilitates the electricity generation and allows the electrons to move away from the photosensitive anode through the external circuit. Therefore, the change in the open circuit potential at the anode decreases with the increasing of the ammonia concentration (in the range from 2.5 wt% to 10 wt%).

ACKNOWLEDGEMENTS

“This publication was developed under an appointment to the DHS Summer Research Team Program for Minority Serving Institutions, administrated for the U.S. Department of Homeland Security (DHS) by the Oak Ridge Institute for Science and Education (ORISE) through an interagency agreement between DHS and the U.S. Department of Energy (DOE). ORISE is managed by Oak Ridge Associated Universities (ORAU) under DOE contract number DE-AC05-06OR23100. This document has not been formally reviewed by DHS. The views and conclusions contained in this document are those of the authors and should not be interpreted as necessarily representing the official policies, either expressed or implied, of DHS, DOE or ORAU/ORISE. DHS, DOE and ORAU/ORISE do not endorse any products or commercial services mentioned in this publication.” This work is also supported in part by the US National Science Foundation (NSF) under Grant Numbers CMMI-1333044 and DMR-1429674.

COMPETING INTERESTS

Authors have declared that no competing interests exist.

REFERENCES

1. Kaneko M, Ueno H, Ohnuki K, Horikawa M, Saito R, Nemoto J. Direct electrical power generation from urine, wastes and biomass with simultaneous photodecomposition and cleaning. Biosensors and Bioelectronics. 2007;23:140.
2. Gan YX, Gan BJ, Su L. Biophotofuel cell anode containing self-organized titanium dioxide nanotube array. Materials Science and Engineering B. 2011;176:1197.
3. Marschall R, Klaysom C, Mukherji A, Wark M, Lu GQ Wang L. Composite proton-conducting polymer membranes for clean hydrogen production with solar light in a simple photoelectrochemical compartment cell. International Journal of Hydrogen Energy. 2012;37:4012.
4. Cheng H, Qian Q, Wang X, Yu P, Mao L. Electricity generation from carboxymethyl cellulose biomass: A new application of enzymatic biofuel cells. Electrochimica Acta. 2012;82:203.
5. Lianos P. Production of electricity and hydrogen by photocatalytic degradation of organic wastes in a photoelectrochemical cell: The concept of the photofuel cell: A review of a re-emerging research field. Journal of Hazardous Materials. 2011;185: 575.
6. Gan YX, Gan BJ, Clark E, Su L, Zhang L. Converting environmentally hazardous

materials into clean energy using a novel nanostructured photoelectrochemical fuel cell. Materials Research Bulletin. 2012; 47:2380.

7. Yin SF, Xu BQ, Zhou XP, Au CT. A mini-review on ammonia decomposition catalysts for on-site generation of hydrogen for fuel cell applications. Applied Catalysis A: General. 2004;277:1.
8. Yin SF, Zhang QH, Xu BQ, Zhu WX, Ng CF, Au CT. Investigation on the catalysis of CO_x-free hydrogen generation from ammonia. Journal of Catalysis. 2004; 224:384.
9. Zhao Y, Wang L, Zhang J, Gong W, Guo H. Decomposition of ammonia by atmospheric pressure AC discharge: Catalytic effect of the electrodes. Catalysis Today. 2013;211:72.
10. Xiao S, Qu J, Zhao X, Liu H, Wan D. Electrochemical process combined with UV light irradiation for synergistic degradation of ammonia in chloride-containing solutions. Water Research. 2009;43:1432.
11. Hill AK, Torrente-Murciano L. In-situ H_2 production via low temperature decomposition of ammonia: Insights into the role of cesium as a promoter. International Journal of Hydrogen Energy. 2014;39:7646.
12. Ma Z, Yang H, Li Q, Zheng J, Zhang X. Catalytic reduction of NO by NH_3 over Fe–Cu–O_X/CNTs-TiO_2 composites at low temperature. Applied Catalysis A: General. 2012;43:427–428.
13. Harara AM, Wang J, Nguyen MJ, Morales KP. Cobalt-doped titanium dioxide photo-electrochemical fuel cells for waste water purification. Journal of Scientific Research & Reports. 2014;3:3068.
14. Kolinko PA, Kozlov DV. Products distribution during the gas phase photocatalytic oxidation of ammonia over the various titania based photocatalysts. Applied Catalysis B: Environmental. 2009; 90:126.
15. Sa J, Aguera CA, Gross S, Anderson J. A photocatalytic nitrate reduction over metal modified TiO_2. Applied Catalysis B: Environmental. 2009;85:192.
16. Yuzawa H, Mori T, Itoh H, Yoshida H. Reaction mechanism of ammonia decomposition to nitrogen and hydrogen over metal loaded titanium oxide photocatalyst. The Journal of Physical Chemistry C. 2012;116:4126.
17. Ou HH, Hoffmann MR, Liao CH, Hong JH, Lo SL. Photocatalytic oxidation of aqueous ammonia over platinized microwave-assisted titanate nanotubes. Applied Catalysis B: Environmental. 2010;99:74.
18. Wan B, Chen MB, Zhou XY, Wang W, Li WG. Photoelectrocatalytic performance of Ag/$TiO_{2-x}N_x$ nanotube. Journal of Inorganic Materials. 2010;25:285.
19. Liu LF, Zhang Y, Yang FL, Chen G, Yu JC. Simultaneous photocatalytic removal of ammonium and nitrite in water using Ce^{3+}–Ag^+ modified TiO_2. Separation and Purification Technology. 2009;67:244.
20. Reli M, Ambrozová N, Sihor M, Matejová L, Capek L, Obalová L, Matej Z, Kotarba A, Kocí K. Novel cerium doped titania catalysts for photocatalytic decomposition of ammonia. Applied Catalysis B: Environmental. 2015;178:108.
21. Ren K, Gan YX, Young TJ, Moutassem ZM, Zhang L. Photoelectrochemical responses of doped and coated titanium dioxide composite nanotube anodes. Composites Part B: Engineering. 2013;52: 292.
22. Wang H, Zhang X, Su Y, Yu H, Chen S, Quan X, Yang F. Photoelectrocatalytic oxidation of aqueous ammonia using TiO_2 nanotube arrays. Applied Surface Science. 2014;311:851.
23. Roy P, Berger S, Schmuki P. TiO_2 nanotubes: Synthesis and applications. Angewandte Chemie. 2011;50:204.
24. Macak JM, Gong BG, Hueppe M, Schmuki P. Filling of TiO_2 nanotubes by self-doping and electrodeposition. Advanced Materials. 2007;19:3027.
25. Ren K, McConell CA, Gan YX, Afjeh AA. Magnetic field enhanced photoelectro-chemical response of a nanostructured titanium dioxide anode. Electrochimica Acta. 2013;109:162.
26. Gan YX, Yazawa RH, Smith JL, Oxley JC, Zhang G, Canino J, Ying J, Kagan G, Zhang L. Nitroaromatic explosive sorption and sensing using electrochemically processed polyaniline-titanium dioxide hybrid nanocomposite. Materials Chemistry and Physics. 2014;143:1431.
27. Askeland DR, Wright WJ. The science and engineering of materials. 7th Edition, Cengage Learning, Boston, MA. 2014;804.

28. Callister Jr WD, Rethwisch DG. Materials science and engineering an introduction. 9th Edition, John Wiley & Sons Inc., Hoboken, NJ. 2014;683.
29. Rieger PH. Electrochemistry. 2nd Edition, Chapman & Hall, New York, NY. 1993; 185.
30. Oldham HB, Myland JC. Fundamentals of electrochemical science. Academic Press, San Diego, CA. 1994;315.
31. Sawyer DT, Sobkowiak A, Roberts Jr JR. Electrochemistry for chemists. 2nd Edition, John Wiley and Sons, Inc. New York, NY. 1995;291.

Peer-review history:
The peer review history for this paper can be accessed here:
http://sciencedomain.org/review-history/14151